Investigation on the Effects of Pavement Material on the Micro-scale Thermal Environment

○ Vu Thanh Ca*, Takashi Asaeda† and Ashie Yasunobu‡

Abstract

A numerical model has been developed for the simulation of the heating and evaporation processes in the urban canopy layer. The three dimensional filtered Navier-Stokes equations, continuity equation and heat and moisture transfer equations in the in the air are solved using a Large Eddy Simulation (LES) technique to obtain the wind, air temperature and moisture fields in the canopy layer. The heat exchange between the roof, walls of buildings, pavement surface and the air is evaluated by solving the heat conduction equation for the roof, walls and pavement. The heat and moisture fluxes at the unpaved ground surface or porous pavement surface are evaluated by the solutions of equations coupling subsurface heat and moisture transfer, and the evaporation at the ground surface.

Using the model, the heating and evaporation process in the urban canopy layer, and its effects on the urban thermal environment can be evaluated.

1 Introduction

It has been well-known that the ground surface in the urban area, where a large portion is usually covered by asphalt and concrete, can act as a heat reservoir to absorb incoming solar radiation during the day, which together with anthropogenic heat released by human activities create the so called urban heat island (Asaeda and Vu, 1993).

Studies (Asaeda and Vu, 1993, Asaeda et al, 1996) have revealed that at noon, surface temperature of asphalt pavement can reach more than 55°C, and the surface releases more than 350W/m^2 and 600W/m^2 to the atmosphere in the form of sensible heat and upward longwave radiation, respectively. The sensible heat directly heats the air, while the upward longwave radiation can increase the thermal load on the pedestrian and cause great thermal discomfort.

The main reason for the increase of temperature at the surface of the normal impermeable pavement is the lack of evaporation, which for natural bare soil surface and at its peak at noon can be as large as 400 W/m^2 and consumes a large portion of net radiation to the surface, helps the surface to reduce its temperature. Due to intensive evaporation, surface temperature of bare soil at noon is only around 40°C and decrease to lower than that of the air soon after sunset (Asaeda and Vu, 1993).

Thus, it is desirable that a kind of pavement which enable the exchange of water between the pavement and the underlying soil, and consequently enable the evaporation at the ground surface be used in the urban area. Previous study (Vu et al, 1996) found that among various porous pavement materials, ceramic porous pavement can be used for this purpose. However, the effects of this and other kinds of pavement on the below-canopy thermal climate has not been properly investigated.

This study presents preliminary attempts to investigate the heating and evaporation processes in the urban canopy, and the effects of different pavement materials on the urban canopy microclimate based on a numerical model. The Navier-Stokes equations, continuity equation, equations of heat and moisture transfer in the air are solved using a Large Eddy Simulation (LES) technique coupling with appropriate boundary conditions for momentum, heat and moisture fluxes at the ground surface and walls and roof of buildings. At this time a simple computational region of the size 120m(length)

*Faculty of Engineering, Saitama University
†Graduate School of Environment and Human Engineering, Saitama University
‡Building Research Institute, Ministry of Construction

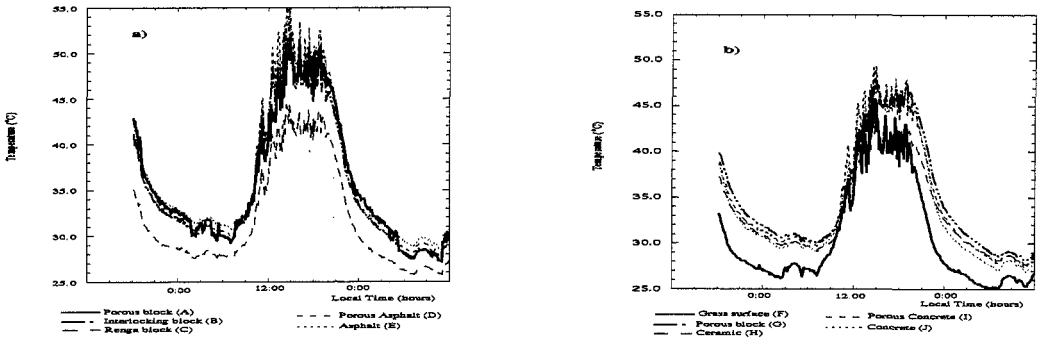

Figure 1: Surface temperature of various pavement samples on August 8-10, 1994

× 120m(width) × 100m(height) is assumed; and a building of the size 20m(length) × 15m(width) × 25m(height) is supposed to be constructed in the computational region. Computations were performed for two cases: the ground surface is covered totally by asphalt and the ground surface is covered totally by ceramic porous pavement.

2 Field Experiment

Outdoor experiments were performed for the purpose of understanding the heating characteristics of various pavement materials. During the field experiment, temperature and ground heat flux at the surface and various depths below surface of ten pavement samples together with meteorological conditions such as air temperature, relative humidity, wind velocity, solar radiation, downward long-wave radiation were recorded at 5 minutes interval continuously from August, 1994 to May, 1995. More information on the experiment can be found in Vu et al (1996).

Surface temperatures of various pavement samples measured during the extensive observation of 8-9 August, 1994 are depicted in Figs. 1 (a,b). As in the figures, at noon, surface temperature of the porous asphalt pavement reaches 52°C, which is almost the same as that of the normal porous block and 3°C lower than that of the asphalt pavement, which reaches 55°C. At the same time, temperature at the surface of ceramic pavement reaches only 42°C, almost the same as that of the surface of the natural grass.

The high surface temperature of the normal porous pavement can be explained by the effects of the pore size in pavement materials on the thermal behaviours of the pavement. The normal porous block, having a large pore, can not keep the water inside and is dried up rapidly. This makes its surface temperature at noon as high as that of the normal impermeable concrete pavement. On the other hand, ceramic porous pavement, possessing small pore can absorb a large amount of water during a rainfall and from the underlying soil. The water contained inside the pavement sample is later evaporated, which helps keeping the temperature at the surface of the ceramic pavement much lower than that at the surface of other porous pavements.

3 Analysis the Effects of Pavement on the Urban Microclimate Based on a LES Model

In order to investigate the effects of heating and evaporation processes at the surface of the ceramic pavement on the urban microclimate, and with the purpose of understanding the heat and moisture transfer processes inside the urban canopy layer, a turbulent model of the Large Eddy Simulation (LES) type has been developed. The outline of the model is as follows

3.1 Governing Equations

A top-hat filter is applied to the Navier-Stokes equations, continuity equation and equations of heat and moisture transfer in the air. The three-dimensional filtered equations with the Boussinesq

approximation after non-dimensionalization can be written in tensor form as follows:

$$\frac{\partial u_i}{\partial t} + \frac{\partial}{\partial x_j}(u_i u_j) = -\frac{\partial p}{\partial x_i} - \frac{1}{R_e}\frac{\partial^2 u}{\partial x_j^2} - \frac{\partial \tau_{ij}}{\partial x_j} + \frac{R_a}{P_r R_e^2 T}\delta_{i3}. \tag{1}$$

$$\frac{\partial u_j}{\partial x_j} = 0, \tag{2}$$

$$\frac{\partial \theta}{\partial t} + \frac{\partial}{\partial x_j} u_j \theta = -\frac{1}{P_r}\frac{\partial}{\partial x_j} H_j, \tag{3}$$

$$\frac{\partial q}{\partial t} + \frac{\partial}{\partial x_j} u_j q = -\frac{1}{P_r}\frac{\partial}{\partial x_j} Q_j, \tag{4}$$

where u is the filtered velocity vector and u_i are its components, ω is the filtered vorticity vector, t time, p filtered pressure, θ and q are the filtered virtual potential temperature and mixing ratio, respectively; $K = |u|^2/2$ the mean kinetic energy, τ_{ij}, H_j and Q_j are the subgrid scale (SGS) Reynolds stresses, heat and moisture fluxes, respectively; R_e $(= Uh/\nu)$ Reynolds number, P_r $(= \nu/\kappa_h)$ the Prandtl number, R_a $(= gh^3\Delta\theta/\nu\kappa_h)$ Rayleigh number and $\Delta\theta = \theta - <\theta>$ with h a characteristic height, U a characteristic velocity, and ν and κ_h the kinematic viscosity and thermal diffusivity of the air, respectively. Here, the angle bracket $<>$ is used to denote the horizontally average values.

In the system of equations (1-4), velocity components are nondimensionalized by wind velocity U at large height, length by a characteristic length h, the total height of the computational domain, which extents to 100m from the ground surface, virtual potential air temperature and mixing ratio by virtual potential air temperature and mixing ratio at the top of the computational domain θ_a and q_a, respectively.

The subgrid-scale (SGS) Reynolds stresses is defined as

$$\tau_{ij} = R_{ij} - \frac{R_{kk}}{3}\delta_{ij} \tag{5}$$

with

$$R_{ij} = \overline{u_i' u_j'} \tag{6}$$

The overbar in equation 6 represents the filter operation. As in equations (5-6) the Leonard stress and the cross terms are neglected.

$$\tau_{ij} = -2\nu_m S_{ij} \tag{7}$$

where the rate of strain tensor S_{ij} is defined as

$$S_{ij} = \frac{1}{2}\left(\frac{\partial u_i}{\partial x_j} + \frac{\partial u_j}{\partial x_i}\right) \tag{8}$$

The most widely used prescription for the subgrid scale eddy viscosity ν_m is the Smagorinsky (1963) nonlinear model.

The SGS heat and moisture flux are evaluated as

$$H_j = -\frac{\nu_m}{P_r}\frac{\partial T}{\partial x_j} \tag{9}$$

$$Q_j = -\frac{\nu_m}{P_r}\frac{\partial q}{\partial x_j} \tag{10}$$

The instantaneous SGS eddy viscosity is evaluated following Moeng (1984)

$$\nu_m = c_s l k^{1/2}, \tag{11}$$

where c_s is a constant, equals to 0.1; and k is the SGS turbulence kinetic energy $k = \overline{u_i' u_i'}/2$. The prognostic equation for k is as follows

$$\frac{\partial k}{\partial t} = -\overline{u_i}\frac{\overline{\partial k}}{\partial x_i} - \overline{u_i' u_j'}\frac{\partial u_i}{\partial x_j} + \frac{R_a}{R_e^2 P_r \Delta T}\overline{w'\theta'} - \frac{\partial[\overline{u_i'(k+p')}]}{\partial x_i} - \varepsilon \tag{12}$$

The closure assumptions made here in order to solve (12) are the downgradient diffusion assumption

$$\overline{u_i'(k+p')} = -2\nu_m \frac{\partial k}{\partial x_i}, \tag{13}$$

and the Kolmogoroff hypothesis

$$\varepsilon = \frac{c_\varepsilon k^{3/2}}{l}, \tag{14}$$

with

$$c_\varepsilon = 0.19 + 0.51 l/l_0, \tag{15}$$

and l, l_0 are length scales of the SGS motion.

3.2 Boundary Conditions and Solution Scheme

The boundary conditions at the ground surface for wind velocity is evaluated following Moeng (1984), i.e. using the similarity formulas. Zero normal gradients of velocity components across the downwind, lateral and upper boundaries are assumed. At the upwind boundary, a turbulent velocity distribution profile in the vertical direction is specified. For the heat and moisture transfer equations (3-4), zero normal gradients of air temperature and mixing ratio are specified at all horizontal open boundaries, and given free atmospheric temperature and mixing ratio at the upper boundary. Temperature at the surfaces of roof, walls of the building is given by integrating a one-dimensional heat conduction equation

The energy budget at the surface elements which determines the boundary conditions for equations (25) and equations for the heat and mass transfer at the ground surface is written as

$$-K\frac{\partial T_c}{\partial x_n} = R_{net} + H + LE \tag{16}$$

where R_{net} is the net radiation to the surface, H and LE are the sensible and latent heat fluxes, respectively. The net radiation to a point on the surface is the sum of direct and diffused solar radiations, shortwave reflection and longwave emission from the surrounding environment and longwave radiation from the sky minus the emission from the surface.

In the numerical model for the coupling between sub-surface transfers of heat and moisture of Asaeda and Vu (1993), the subsurface distribution of temperature and matric potential were computed. Then, the vapor density (mixing ratio) at the ground surface is evaluated with the known

temperature and matric potential based on the assumption of the equilibrium between the liquid phase and the vapor phase in the soil pore.

The system of equations (1-4) for the wind velocity, air temperature and vapor density fields was discretized in finite volume form on a non-uniform, non-staggered grid as that of Armfield (1991) Vu et al (1995). Pressure is computed using the SMAC method.

For the three-dimensional turbulence, the grid mesh of a LES model should fall within the inertial subrange. The model proposed by Moeng (1984) and employed in this study is generally not superior than the modified Smagorinsky model. However, for this kind of model, since the SGS turbulent kinetic energy is computed explicitly, no equilibrium assumption is required. This would allow a grid mesh much larger than the length scale of the inertial subrange.

However, since a strong shear flow is expected in the computational domain, a fine mesh should be much desirable. In this paper, a mesh of 37(lateral)×38(longitudinal)×44(vertical) is used. The mesh can be clearly seen in Figs. 2.

Since a small time step is needed for the computation of the turbulent field, the computation, at this stage, unsteady computation is still no possible. Thus, the results presented in this paper is only that for the steady state. The initial conditions for air temperature, wind velocity, wall and ground surface temperature in each computation is taken from that computed using a static pressure model reported in Vu et al (1995) and the computation is perfomed until the steady state is reached.

3.3 Results and Discussions

Figs. 2(a-d) depict the horizontal distributions of air temperature and wind velocity at 2 p.m. and 8 p.m. for the cases that the ground surface is covered by ceramic and asphalt pavements, respectively. Figs. 2(e,f) depicts the air temperature and wind velocity distribution at a vertical cross-section at the center of the computational region at 2 p.m. for the cases of asphalt pavement surface and ceramic pavement surface, respectively. From the computational results, it is clear that results of this model for the wind velocity is very similar to that of other models for the computation of wind velocity field around buildings and that obtained from wind tunnel experiments (Murakami et al, 1991). However, as in Fig. 2(e,f), height of the wake just behind the building is much higher than that predicted by the numerical model of Murakami et al (1991) and much more close qualitatively to the results of the wind tunnel experiment results (Fig. 1 of the same paper). As in Figs. 2(a-d), it is clear that in generall, two large eddies are formed at the two edges of the building, carried downstream by the mean flow where turbulent energy is dissipated. In this computation, due to a strong wind (2m/s at the top of the computational region) and a small computational area, turbulent is mainly generated by the wind shear, and the contribution of the bouyancy is rather small. Thus, flow patterns around buildings are almost the same for all cases. From the horizontal distribution of air temperature, it can be seen that two hot regions are observed at the two edges of the building. This is because of the evolution of eddies, upward flows are observed at the to edges of the building while downward flow is observed at its center. The upward flow bring up the near-surface hot air while downward flow bring down cool air from above. The downward flow at the center of the building can be clearly seen in Figs. 2(e,f).

At noon, as depicted in Figs. 2(a,b), the air temperature at 3.5m above the surface for the case of asphalt pavement surface is in general about 1.5K higher than that for the case of ceramic pavement surface. For the hottest region near two edges of the building, this difference is amounted to more than 2.5K. At 8 p.m., this difference is about 1K as depicted in Figs. 2 (c,d). Fig. 2(d) shows that air temperature are almost homogeneous horizontally for the case of ceramic pavement surface. This is because the ceramic pavement surface has been cooled down and its temperature is nearly equal to that of the air.

Figs. 2(e-f) give pictures of vertical distribution of air temperature at the cross-section at the center of the building. The figures show that for two cases, two hot regions are observed near the roof, which is heated extensively from the morning, and near the ground surface. However, near the ground surface, air temperature above ceramic pavement is about 2K lower than that above the asphalt surface.

The above finding indicate that significant improvement of the urban micro-scale thermal environment can be achieved if ceramic pavement surface is used.

The accuracy of the proposed numerical model should be check by wind tunnel experiment data

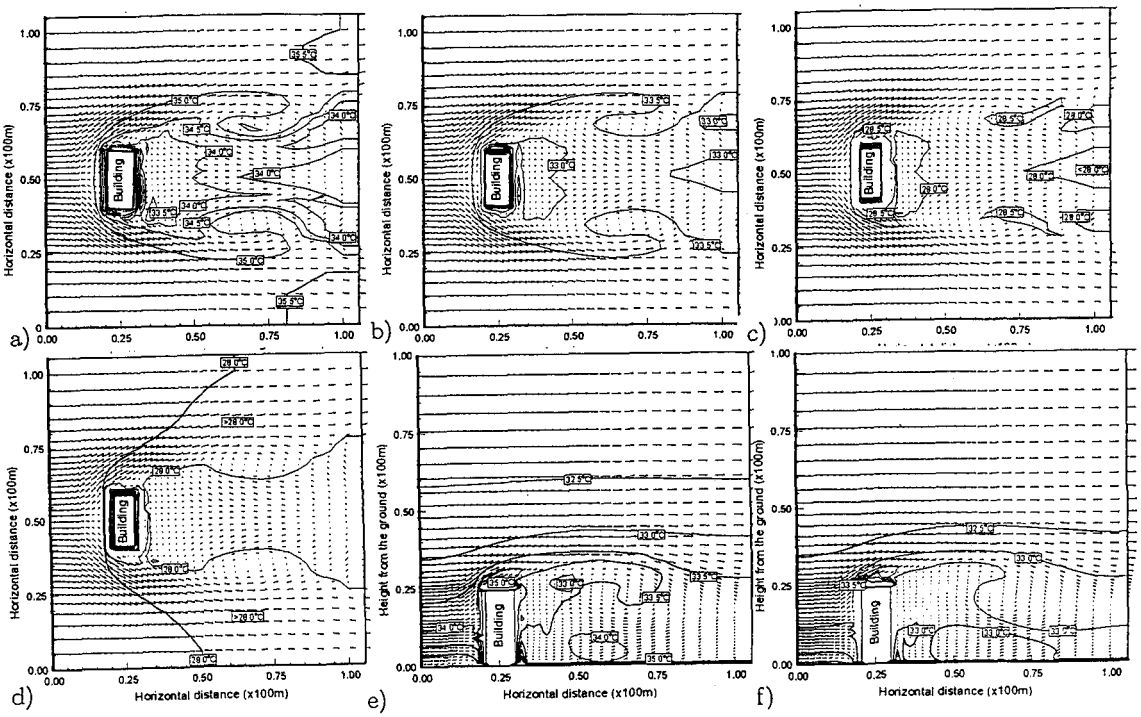

Figure 2: Air temperature and wind velocity at 3.5m above the surface of a) asphalt pavement (2 p.m.), b) ceramic porous pavement (2 p.m.), c) asphalt pavement (8 p.m.), d) ceramic porous pavement (8 p.m.); and air temperature and wind velocity at a vertical cross-section at the center of the computational region at e) asphalt pavement (2 p.m.), f) ceramic porous pavement (2 p.m.).

and the analysis of the sensitivity of the model results to the grid mesh. This will be our future work.

References

Armfield S.W. (1991) Finite difference solutions of the Navier-Stokes equations on staggered and non-staggered grids. *Computers Fluids.* **20**, 1-17.

Asaeda T., and Vu T. C. (1993) The subsurface transport of heat and moisture and its effects on the environment: a numerical model. *Boundary-Layer Meteorol.* **65**, 159-179.

Asaeda T., Vu T. C. and A. Wake (1996) Heat storage of pavement and the effects on the lower atmosphere. *Atmospheric Environment*, **30**, 413-427.

Moeng, C.H. (1984) A large-eddy-simulation model for the study of planetary boundary-layer turbulence. *J. Atmos. Sci.* **41**, 2052-2062.

Murakami S., A. Mochida, Y. Hayashi and K. Hibi (1991) Numerical simulation of velocity field and diffusion field in an urban area. *Energy and Building* **15-16** (1990/91) 345-356.

Smagorinsky J. (1963) General circulation experiments with the primitive equations, I. The basic experiment. *Monthly Weather Review* . **91**, 99-164.

Vu T. C., T. Asaeda, M. Ito and S. Armfield (1995) Characteristics of wind field in a street canyon.*J. Wind Eng. Indust. Aerodynamics.* **57**, 63-80.

Vu T.C., T. Asaeda, T. Fujino and M. Murakami (1995) Effects of greening on the climate of Tama New Town.*Environmental System Research*, Vol. 23, 223-228.

Vu T. C., T. Asaeda and M. A. Eusuf (1996) Utilization of moisture transfer inside porous pavement for the mitigation of thermal effects of paved surface in summer. *Annual Journal of Hydraulic Engineering, JSCE*, 449-454.